14

Molecular Dynamic Simulation of Short Order and Hydrogen Diffusion in the Disordered Metal Systems

Eduard Pastukhov, Nikolay Sidorov,
Andrey Vostrjakov and Victor Chentsov
Institute of Metallurgy, Russian Academy of Sciences, Ural division
Russian Federation

1. Introduction

Main concepts of Hydrogen permeability (HP) mechanism for the pure crystal metals are already stated. There are well-founded theoretical models and numerous experimental researches. As far as disordered systems (in which Hydrogen solubility is much more, than in crystal samples) are concerned, such works appear to be comparatively recent and rare. Particularly, they are devoted to Hydrogen interaction of with amorphous structures. Deficiency of similar researches is caused by thermo-temporal instability of amorphous materials structure and properties.

Unlike crystal alloy, where interstice volumes are presented discretely only by tetrahedron and octahedron cavities, small and big interstice cavities distribution in an amorphous alloy is close to Gaussian function (Polukhin and Vatolin, 1985, Polukhin et.al, 1984, 1986). Thus Hydrogen energy distribution function form in the amorphous alloys cavities is close to the main RDF peak which is approximated by Gaussian function. Inter-cavities transitions are strongly correlated, and the stationary states contribution to the Hydrogen atoms motion is negligible.

Amorfizator-elements (Si, B, C, etc.) insertion into the amorphous metals reduces number of large cavities (octahedrons) providing most energetically favourable Hydrogen migration path. It reduces metal absorption ability, as well as hydrogen diffusion motion intensity, reducing Hydrogen permeability.

Amorphous alloys absorption ability of hydrogen is defined by number and size of cavities for hydrogen insertion, as well as the hydride forming elements (Ti, Zr, Hf, etc.) content in an alloy. Hydrogen diffusion factor in the amorphous alloys depends on its concentration.

Crystal and amorphous Palladium alloys are widely used in membranes for high pure Hydrogen producing. Literary data analysis shows possibility of filtering alloys production for hydrogen based on less expensive metals: V, Nb, Zr, Ta, etc., characterized by high Hydrogen solubility, which defines alloy Hydrogen permeability by diffusion factors as well as Palladium. Negative effect of these elements hydrides formation should be inhibited

by the other metals additives. In the plasma-arc (PAM) and electron beam (EBM) refining melting of the Nb, Zr, Ta, etc. metals, the necessity of impurity elements (especially hydrogen and iron) transport research in such melts arises. Electric and magnetic fields affect to liquid metal and its impurities during melting have been indicated in the number of researches as well.

Therefore research of an electric field intensity affect to the impurity elements transport properties in the liquid metals is very urgent.

Amorphous and liquid systems based on Fe, Pd, Zr, Ta, Si with and without Hydrogen researches are presented in this work. Short order structure experimental results and molecular dynamics simulations are considered. Partial structure factors, radial distribution function of atoms, its mean square displacement and diffusion factors are calculated. Hydrogen concentration affect to its mobility and short order parameters in the system are analyzed. Electric field intensity affect to liquid metals are compared with literary data on impurities removal from Zr and Ta in plasma-arc melting in the Hydrogen presence.

2. Molecular dynamics calculation method

Molecular dynamics method (MD) had been primary proposed in (Alder & Wainwright, 1959). The method allows particles real-time motion analysis using classic equations. So far it's the only numeric method for dens medium dynamic research. Generally accepted nowadays MD calculation scheme is the following. A system consisting of several hundred particles with the given interparticle interaction potential is considered. Classic equations of the particles motion are numerically resolved using Verlet algorithm (Verlet, 1976). It calculates i-particle coordinate on the following (k+1)-step by coordinates on given k- and previous (k-1)-steps.

$$r_i(k+1) = 2r_i(k) - r_i(k-1) + \frac{F_i(k)(\Delta t)^2}{m} \tag{1}$$

Where r_i – radius-vector of particle, m - its mass, F_i – resultant force and Δt – time step. Velocity doesn't take part in calculation. Other algorithms of motion path calculation are considered in (Polukhin & Vatolin 1985). Periodic boundary conditions are used in motion equation solution, i.e. if some particle with p_i - momentum exits through cube face, then other particle with the same momentum enters through opposite face symmetric relatively plane in the center of cube. Interaction in the MD models is defined as the pair interaction potentials resultant force in the pair approximation models. Temperature of system is defined basing on its total kinetic energy. Diffusion factors are calculated from mean square displacement of the particles in model $\left\langle r_i^2(t) \right\rangle$ by the major of steps.

$$D = \frac{1}{6t} < r_i^2(t) >, \tag{2}$$

Where $<r^2(t)>$ – mean square displacement of Hydrogen atoms at t – time.

Disorder systems short order is characterized by of radial distribution function of atoms g (r) (RDF) and its Fourier transform – structure factor s(k). Radial distribution function RDF

determines location probability any atom at r distance from the chosen atom and described in MD model by the well-known formula:

$$g(r) = \frac{(\Delta N)L^3}{4\pi r^2 \Delta r N}, \tag{3}$$

Where ΔN — number of particles in a spherical layer thickness Δr on r distance from the chosen particle: L — cube edge length of basic cell and N — number of its particles. Structure factor s(k) is defined by following equation:

$$s(k) = 1 + \frac{4\pi N}{L^3} \int_0^{r_m} [g(r) - 1] \frac{Sin(kr)}{kr} r^2 dr, \tag{4}$$

Where k is wave vector, $k = (4\pi \text{ Sin } 2\Theta)/\lambda$ and r_m is RDF attenuation radius.

Minimum k value in the MD – experiment is inversely proportional to main cube edge and calculations for smaller k, have not physics sense. Final configuration for RDF in our calculation was chosen its constant value. This condition needs no less than 10000 steps. Coordination number had been calculated by following formula:

$$Z = \frac{4\pi N}{L^3} \int_0^{r_m} g(r) r^3 dr \tag{5}$$

Molecular dynamics calculation had been done using microcanonical (NVE) ensemble.

The particles of system were randomly distributed in the basis MD – cell. Interpartial potentials and its numerical value factors had been taken from works of (Varaksin & Kozjaychev, 1991, Zhou et.al, 2001, Rappe et.al, 1992). General questions of this method using had been considered in details by authors (Polukhin & Vatolin, 1985).

3. Hydrogen in amorphous and recrystallized Fe-Ni-Si-B-C-P alloy (experiment)

Experimental researches of Hydrogen absorption affect to structure and physical-chemical properties of transition metals (Palladium and Iron) alloys are presented by works (Pastukhov et.al, 1988). This researches indicated, that Hydrogen absorption leads to considerable shift of structure relaxation start and finish to the higher heating temperature interval. This process provokes significant modification of the amorphous (Iron based) material strength properties and leads to increased embrittlement. All mentioned changes are adequately displayed on the atoms distribution curves (fig. 1), obtained from diffraction experiment data (Vatolin et.al, 1989).

Hydrogen permeability of the amorphous and recrystallized Fe based ($Fe_{77.333}Ni_{1.117}Si_{7.697}B_{13.622}C_{0.202}P_{0.009}$) alloy membrane (25 micron thickness) was researched by stationary stream method (Pastuchov et.al, 2007). Recrystallized alloy was prepared by vacuum annealing at 400^0C from amorphous specimen.

Molecular Hydrogen injection to input side of degasified specimen at maximal acceptable temperatures (300°C for amorphous and 400°C for recrystallized specimens) didn't lead to

noticeable output stream increase. At 10 torr Hydrogen pressure the stream achieved $3.8 \cdot 10^{12}$ sm^{-2}/s value. Hydrogen medium glow discharge had been used in order to delete the specimen passivation layer. Hydrogen ions, formed in glow discharge, simply penetrate to the specimen bulk (Lifshiz, 1976). We observed significant penetrating stream in this procedure. All researches have been carried out at 2 torr Hydrogen pressure, when the discharge is most stable.

Temperature dependences of the stable (stationary) Hydrogen stream had been defined for amorphous and recrystallized specimens. Lower limit of the researched temperature interval was defined as reliable stream registration possibility which had been stated as 125^0C for amorphous and 200^0C for crystal specimens. Most impotent difference between two states of the researched alloy is observed as non-monotonic output stream increase at temperature expansion in amorphous state.

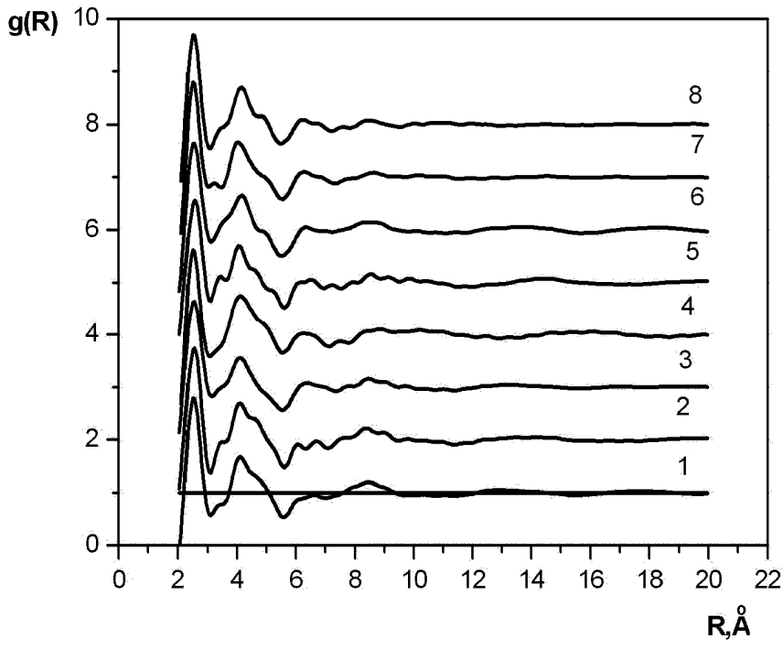

Fig. 1. Atoms radial distribution for amorphous ($Fe_{77.3}Ni_{1.1}Si_{7.7}B_{13.6}C_{0.2}P_{0.009}$) alloy with Hydrogen ($<H_2>$) and Hydrogen absence (1 - 275^0C; 2 - 300^0 + $<H_2>$; 3 - 425^0C; 4 - 425^0C + $<H_2>$; 5 - 450^0C; 6 - 475^0C +$<H_2>$; 7 - 550^0C; 8 - 575^0C +$<H_2>$).

Hydrogen stream stabilization has different nature in amorphous and recrystallized specimens. But both situations are characterized by rapid increase of output stream with characteristic 30÷60s stabilization times.

Amorphous membrane is characterized by very elongated hydrogen output with 6000s stabilizing time after rapid output increase at temperatures from 125^0 C up to 225°C. Hydrogen stream dependence on inverse temperature is illustrated by fig.2. The dependence isn't monotonous and has maximum in 200°C region.

The stream increases from 125^0C and achieves maximum $3.3 \cdot 10^{13}$ $sm^{-2}s^{-1}$ value at 200°C. Subsequent heating demonstrates anomalously sharp decrease. Second specimen follows to classic Arrhenius dependence with activation energy 17.9 kj/mol and maximum stream

value $2.7 \cdot 10^{13}$ $sm^{-2}s^{-1}$ at 375^0C (fig. 2). Amorphization of the alloys leads to considerable free volume increasing, which increases Hydrogen permeability, solubility and diffusion. Special attention should be directed to the Hydrogen permeability changing (by order) effect with comparatively low solubility increase. This effect is explained by competition from amorphization-elements, which occupy large Bernal polyhedron-cavities, first of all in the high amorphization-elements concentration region (Polukhin et.al, 1997). "Overextended" stream yield to the stationary value evidently related to reversible diffusant capture (Herst,1962). Thus Hydrogen escape probability from the traps increases faster than capture probability. It was experimentally showed, that at temperature increase up to 200^0C, low increase Hydrogen streams observed in reality. Its decrease begins after 200^0C. Such behavior is proper namely for the traps with activation energies of escape and capture $E_{esc}>E_{cap}$.

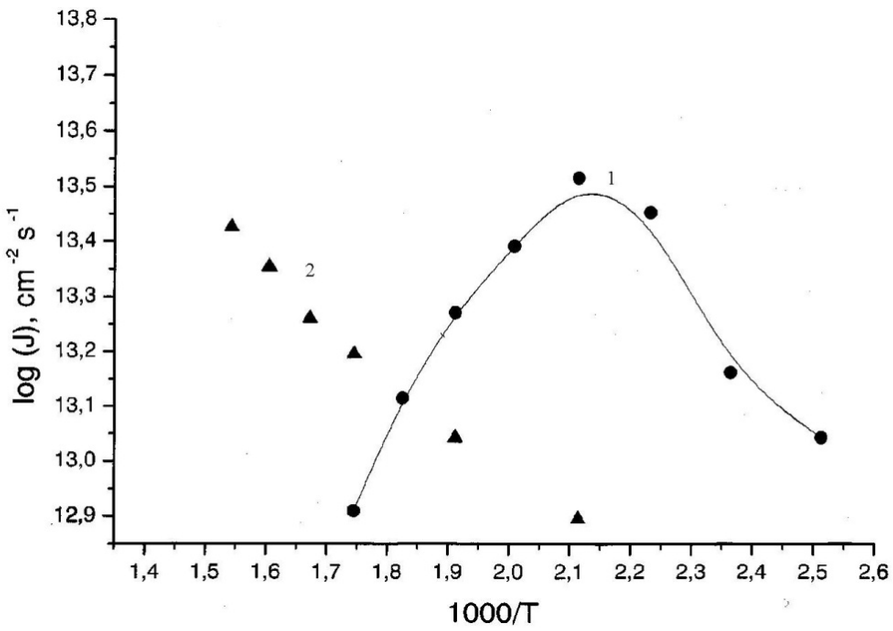

Fig. 2. Stationary Hydrogen stream (J) dependence on temperature. (1 – amorphous alloy, 2 – recrystallized alloy)

Penetrating stream decreasing in amorphous specimen for temperature interval from 200^0 C up to 300^0 C most probably is related to surface processes. Since penetrating stream is three orders less than incident stream to input surface ($V_f \approx 10^{16} cm^{-2}s^{-1}$), balance of streams is written as

$$V_f = V_T + V_r \tag{6}$$

where $V_T + V_r$

$$V_r = V_f C_i / C_{max} \quad \text{and} \quad V_T = b_i \cdot \exp(-E_i/RT) C_i \tag{7}$$

are streams of ion-induced reemission and thermal desorption on input side. Term C_i is Hydrogen concentration in no-violated alloy structure near input surface, b_i – pre-exponent factor. Maximal obtainable concentration in near-surface layer C_{max} at room temperature

(when thermal desorption is negligible) is estimated as 10^{18} at/cm^3 (Grashin et.al, 1982, Sokolov et.al, 1984). In assumption, that C_2 – concentration n on output side much less than C_i, for stationary penetrating stream, we obtain following expression

$$J = A \cdot \exp(-E_d/RT)/(1 + B \cdot \exp(-E_i/RT)) \quad (8)$$

where E_d – diffusion activation energy. The rates of diffusant capture and release are equal in stationary state and do not affect to stationary stream intensity. Thus equation (8) doesn't include interaction parameters of Hydrogen with traps. Approximation results are displayed by solid curves at fig. 3. Energy values E_d^{am} = 40.8, E_i^{am} = 86.7 kj/mol for amorphous, and E_d^{cr} = 71.2, E_i^{cr} = 51.7 kj/mol for crystal specimens give good agreement with experiment data.

Concentration calculation on input membrane side by (6) and (7) equations accounting thermodesorption activation energies is illustrated by fig. 4. Parameter C_{max} , used in calculation does not any effect to activation energies, but affects only to pre-exponent factors.

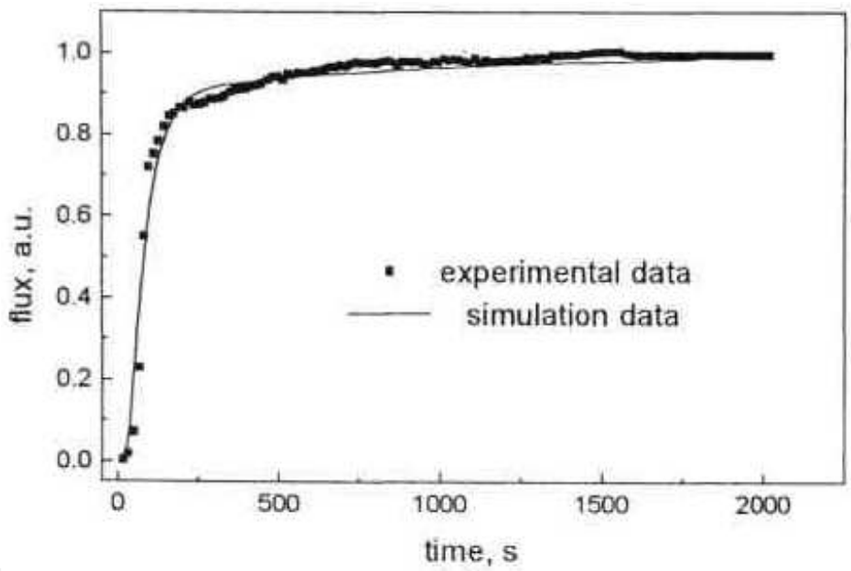

Fig. 3. Stable (stationary) Hydrogen stream through amorphous membrane.

Surface processes and correlation of E_d and E_i values define stationary stream temperature dependence. Concentration C_{am} for an amorphous alloy has C_{max} value up to 175°C temperature and penetration rate is defined by diffusion, at that stream increases. Following temperature increase leads to exponential C_i concentration decrease, and $E_d < E_i$ correlation leads to stream decreasing. Input C_{cr} concentration for recrysallyzed alloy decreases in all temperature interval (fig. 4, curve 2), and $E_d > E_i$ relation leads to classic Arrhenius dependence

$$J \approx \exp(-E_a/RT) \quad (9)$$

where $E_a = E_d - E_i \sim 19.6$ kj/mol in our calculation, that is close to E_a = 17.9 kj/mol, obtained experimentally.

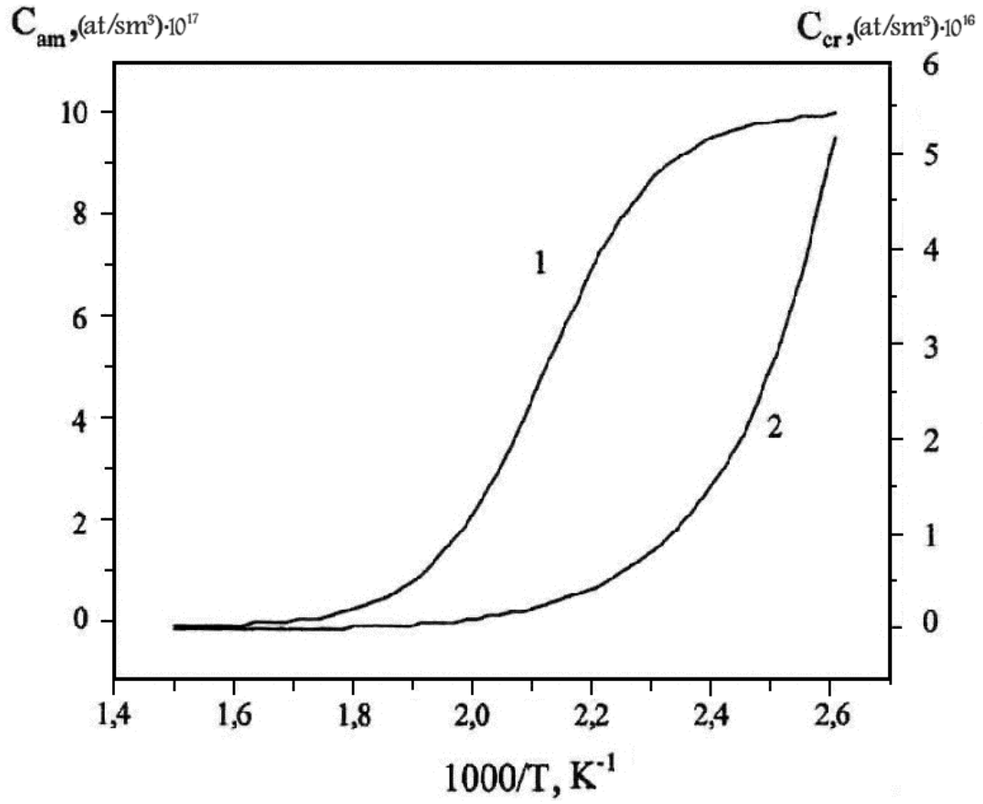

Fig. 4. Temperature Hydrogen concentration dependence at input side of membrane (1- amorphous alloy, 2- recrystallized alloy).

Diffusion activation energies related to specimens structure, obviously. Excess free volume presence in the amorphous alloy provides less energy consumption for the Hydrogen atom jumps from one interstice to another. Besides some part of interstices may perhaps be wrong Bernal cavities, i.e. be deformed. Thermodesorption activation energy in recrystallized alloy is less than in amorphous one $E_i^{cr} < E_i^{am}$. This fact could be explained by surface reconstruction and changing of the passivation layer to the Hydrogen desorption.

4. Hydrogen effect to the short order structure for liquid, amorphous and crystal silicon

Due to its semiconductor properties, Silicon had been found wide application in the recent microelectronics and electronic technique. Hydrogen has been generally recognized to play impotent function in the different complex formation in the amorphous Silicon. Attention to the Hydrogen behavior in Silicon is explained by its affect to physical-chemical properties, which gives opportunity of new materials with necessary properties development.

Hydrogen diffusion in crystal Si was researched by TBMD (tight binding molecular dynamics) method (Panzarini. & Colombo, 1994). The model considered single Hydrogen atom in 64-atoms super-cell of Silicon. On the TBMD data the authors supposed, that

Hydrogen diffusion mechanism in crystal Silicon acts according to Arrhenius low, and there are not other "anomalous" mechanisms but, for example, the single skips. Amorphous Silicon short order structure had been researched in the works of (Pastukhov et.al, 2003, Gordeev et.al, 1980). It had been found, that amorphous Silicon retains covalent bond type with coordination number Z=4.2, in difference with melt, where the bond has metallic character (Z=6.4).

The data of experimentally estimated values for Hydrogen diffusion factors in amorphous Si are limited, and published results are not in good agreement. The experimental research data on amorphous Silicon Hydrogen permeability are presented in the work (Gabis, 1997). For Hydrogen transfer through amorphous Silicon film the author used model, where besides diffusion, low rate of the processes on surface, as well as capture and temporal keeping of the Hydrogen diffusing atoms in traps had been taken into consideration. It's the author's opinion that Hydrogen transfer related to local bonds Silicon-Hydrogen reconstruction.

Physics-chemical properties of computer models (containing thousands atoms) for amorphous Silicon, could be described in terms of empiric potentials (Tersoff, 1986, Stillimger & Weber, 1985).

We used interparticle potential (Tersoff, 1986) and MD method to calculate structure parameters and diffusion factors of Si and H in crystal, amorphous and liquid Silicon (Pastukhov, 2008).

Calculations had been carried out for system, containing 216 Silicon and 1 Hydrogen atoms in basic cube using periodic boundary conditions. Cube edge length had been had been taken according to experimental density system under consideration at 298K temperature. Molecular dynamic calculation results are presented on fig. 5, 6 and in table 1. Valent angles mean values were found from first and second coordination sphere radii using following formula:

$$\varphi = 2\arcsin\left(\frac{r_2}{2r_1}\right) \tag{10}$$

Experimental data analysis obtains, that, in certain approximation, there is one metastable equilibrium configuration of atoms with coordination number 4 in the c-Si *и* a-Si materials with Hydrogen as well as without it. First peak sharpness of intensity curve (fig. 6) indicates comparatively large ordering in a-Si. First and second maxima of RDF curve practically coincide. Differences are observed in consequent part of curves. Third maximum of RDF for a-Si is practically absent.

Computer calculations for Si-H model found, that Hydrogen diffusion mechanism in crystal Si with n – conductivity type is realized by electro-neutral Hydrogen atoms migration through tetrahedral interstices according to the same principle as screened proton diffusion in the amorphous transition metals (Vatolin et.al, 1988). However Hydrogen atom moving path trough matrix nodes accompanied by Si-Si bond breakage due to Si atom 0.05nm shift from the node occupied and formation of chemical bond Si-H and free Si bond, left in the lattice node.

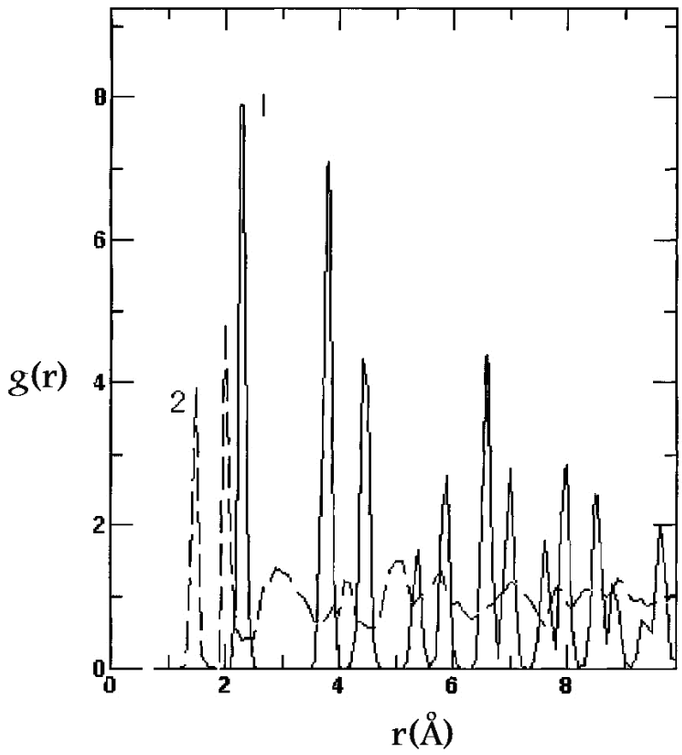

Fig. 5. RDF of the Si-Si (1) and Si-H atoms (2) for crystal Silicon with Hydrogen at 278K.

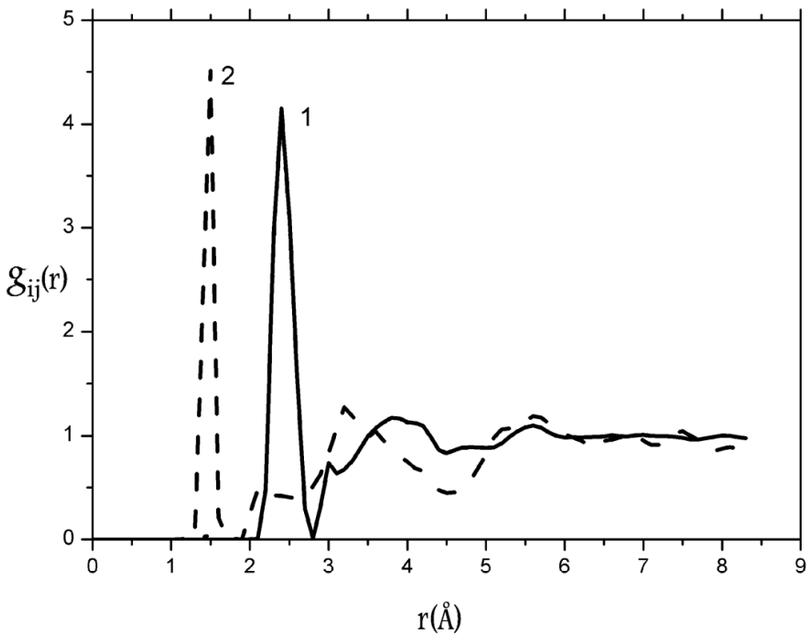

Fig. 6. RDF of the Si-Si (1) and Si-H atoms (2) for amorphous Silicon with Hydrogen at 278K.

Silicon phases structure	RDF Peaks positions, Nm.		Coord. numb. Z	Mean angle inter-bonds φ	Diff. factors D, cm^2/s	Density ρ, g/cm^3.
	r_1	r_2				
1	2	3	4	5	6	7
Diamond	0,236	0,384	4			
White Tin (calculation)	0,25	0,355; 0,42	6,3			
Liquid Si (1700K)			6,4	103,9±26,8	$6,4 \cdot 10^{-5}$	
a-Si (300K)	0.241		4.6	106.3±21		2.294
a-Si, (298K) Our data MD-model	0.240	0.386	4,2	106		2.10
a-Si+H, (298K) Our data MD-model	(Si-Si) 0,250 (Si-H) 0.15	(Si-Si) 0.450 (Si-H) 0.218	4,2	(φ_{Si-Si}) 180 (φ_{Si-H}) 90	D_{Si} $1.94 \cdot 10^{-5}$ D_H $4.83 \cdot 10^{-4}$	2.10
c-Si+H, (298K) Our data MD-model	(Si-Si) 0,231 (Si-H) 0.15	(Si-Si) 0,380 (Si-H) 0.215/0.27	4	(φ_{Si-Si}) 110 (φ_{Si-H}) 90	D_{Si} $2.45 \cdot 10^{-6}$	2.33

Table 1. Short order parameters for crystal (c-Si), liquid (l-Si) and amorphous Silicon (a-Si). (Pastukhov et.al, 2003, Gordeev et.al, 1980).

5. Hydrogen diffusion in the amorphous Pd-Si alloy

Model system (Pastukhov et.al, 2009), used in MD method for Hydrogen behavior research in the amorphous Pd-Si alloy at T=300K temperature, was presented by 734 Palladium particles, 130 Silicon particles and 8 Hydrogen particles in the cubic cell with 2.44869nm edge length. Motion equation integration was carried out with $1.8 \cdot 10^{-15}$s time steps. Short order structure analysis of the amorphous Pd materials (Sidorov & Pastukhov, 2006) and Pd-Si (15 ат.%) with Hydrogen had been carried out using partial functions $g_{ij}(r)$ of Pd-Pd, Pd-Si and Pd-H pairs (Pastukhov et.al, 2009) (fig. 7 and 8).

Second peak of $g_{ij}(r)$ curve for Pd-H (fig. 7) has change symmetry shoulder in comparison with $g_{ij}(r)$ curve for Pd-Pd.

Refer to (Herst, 1962), distances, related to second g(r) peak are formed by 3 types of contact: a) two Pd atoms through Pd atom ($r = 2r_0$); b) two Pd atoms trough через two Pd atoms ($r = 1.732r_0$); c) two Pd atoms through three Pd atoms ($r = 1.633r_0$). More easy Hydrogen affected turns contact of Pd-Pd atoms, realized by b) - type. Amorphous Palladium structure changes, due to Hydrogen presence, are caused by re-distribution of formed distances to its increasing (right sub-peak of RDF second peak). Observed second peak splitting inversion of $g_{ij}(r)$ for amorphous Palladium with Hydrogen obtains information about short order reforming of metal. Second peak differences of $g_{ij}(r)$ for Pd-Pd and Pd-H indicate strong Hydrogen affect to Palladium matrix structure.

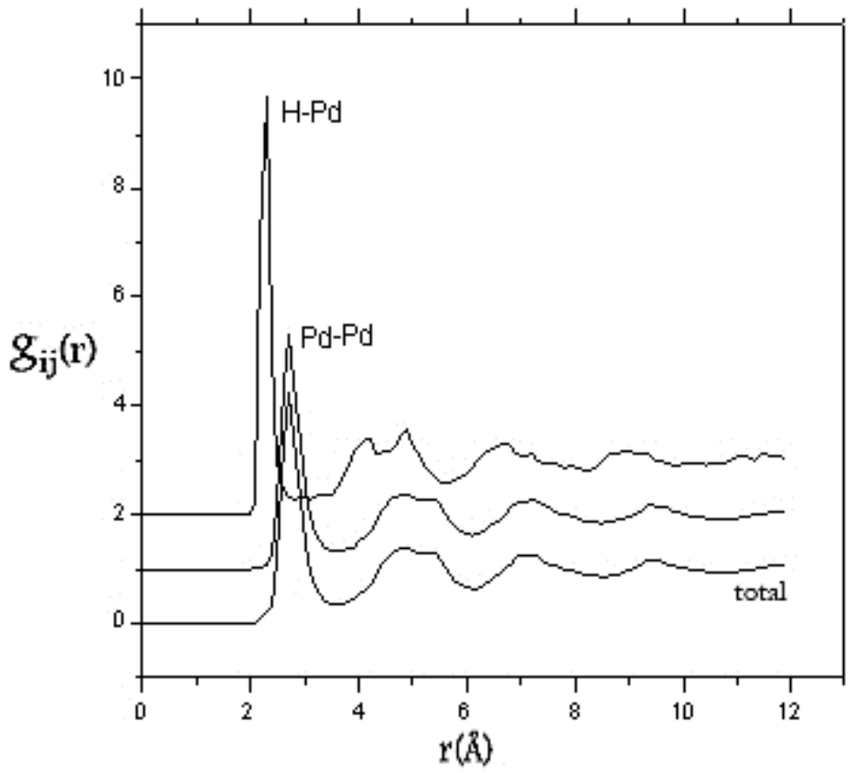

Fig. 7. Partial RDF in an amorphous Pd-H – system.

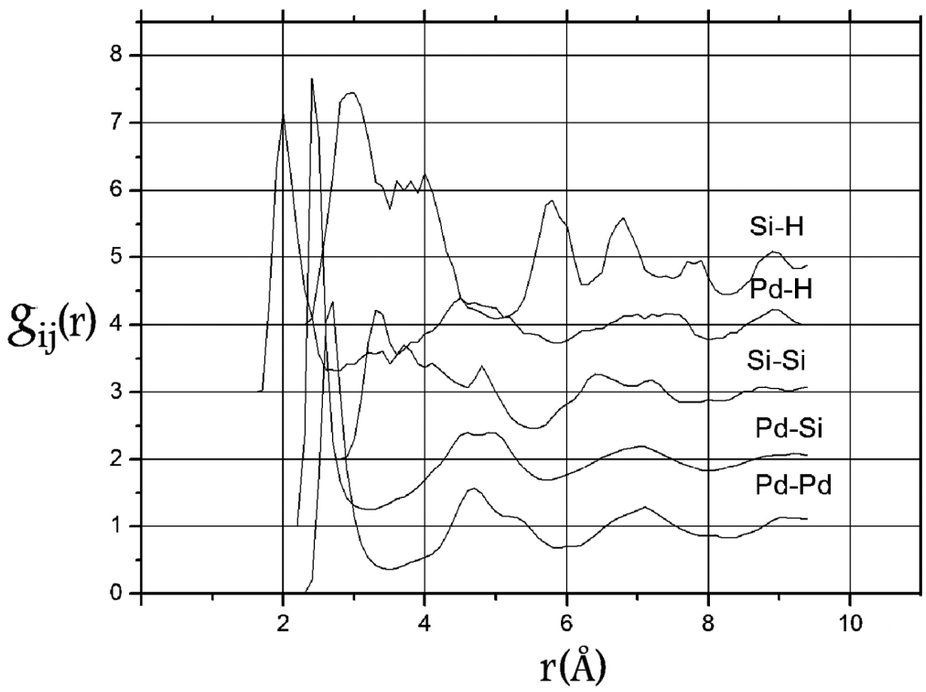

Fig. 8. Partial RDF for amorphous Pd-Si (15 at.%)-H alloy.

Partial RDF for Si-Si indicates to preferential Silicon atoms distribution relatively each other in the second coordination sphere, i.e. Palladium atoms cover Silicon atoms by the first coordination shell (fig. 8).

The effects observed in MD – model allow assumption about micro-grouping presence, which are identified as stable hydride structures, indicating to high degree of dissipative structures of Pd-H, Si-H - types presence (Ivanova et.al,, 1994, Avduhin et.al, 1999).

Hump, observed close to 3.44nm^{-1} (fig. 9) on our calculated and experimental (Polukhin 1984) structure factor curves for amorphous state with Hydrogen as well as its absence, hasn't so far interpretation. Authors (Polukhin & Vatolin, 1985) have shown by statistic geometry method, that most often Voronoy-polyhedrons occurred in the amorphous metals are recognized as polyhedrons with 12, 13, 14, 15 coordination numbers for given sties-atom.

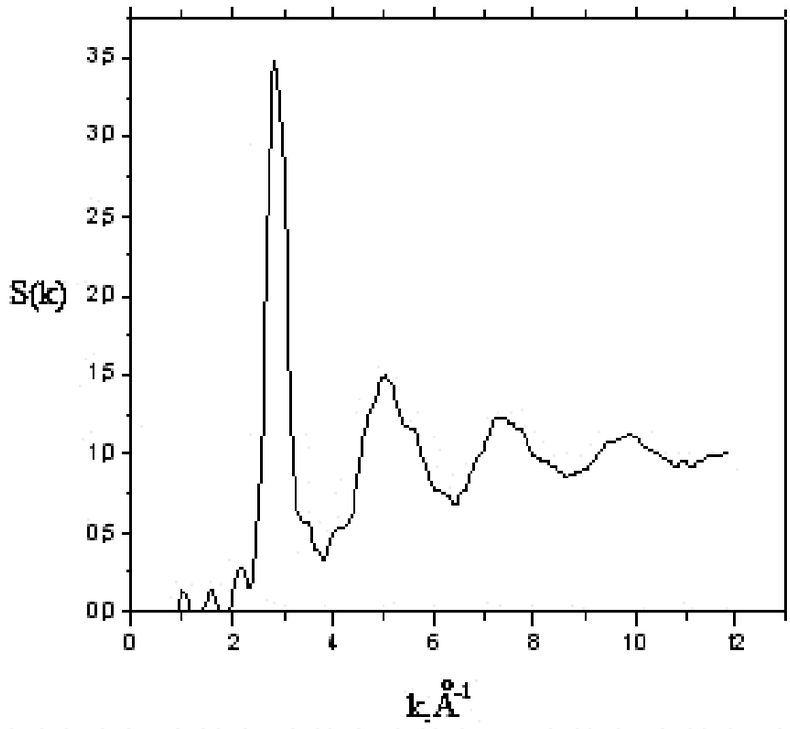

Fig. 9. Structure factor for amorphous Pd-Si with Hydrogen obtained by MD – model calculation.

Mixed type micro-groupings occurred, in $Pd_{85}Si_{15}$ alloy, are formed with most presence of BCC and FCC polyhedron type. Particles number does not exceed 13-14 in one cluster.

Amorphous Pd-Si alloy structure model is supposed to consist from Palladium micro-groupings, characterized by distorted triangle pyramid form with 2.5Å leg (Pd-Si) and regular 2.71Å leg (Pd-Pd) base triangle (Polukhin, 1984)

Separately chosen Pd, Si and H atoms motion in our model is different by its character.

Calculated diffusion factors values for Pd-H system were: $D_H = 18.8 \cdot 10^{-6}$ cm^2·s^{-1}, $D_{Pd} = 3.4 \cdot 10^{-6}$ cm^2·s^{-1}, and $D_H = 6.67 \cdot 10^{-6}$ cm^2·s^{-1}, $D_{Pd} = 2.0 \cdot 10^{-6}$ cm^2·s^{-1} for amorphous Pd-Si-H alloy.

As MD model calculation show, not only Silicon atoms can affect Hydrogen mobility, but Hydrogen itself can change considerably diffusion of the other components of alloy. For example, Pd-Si system without Hydrogen has $D_{Si} = 4.93 \cdot 10^{-6}$ cm$^2 \cdot$s^{-1}, but $D_{Si} = 2.53 \cdot 10^{-6}$ cm$^2 \cdot$s^{-1} with Hydrogen presence. There are different energy zones in an amorphous system, which lead to different time mode of Hydrogen diffusion.

Therefore low of defunding particle energy change in the amorphous metals should be statistic nature and be defined by the cavities type distribution type. Due to little part of the octahedron cavities, three types of diffusion process are possible in the amorphous metals. That are octahedron-octahedron, octahedron-tetrahedron-octahedron, octahedron-octahedron, tetrahedron-tetrahedron. Due to volume changing in the hydrogenization process for crystal is similar to that for amorphous alloys (Kircheim et.al, 1982), this fact indirectly proves, that hydrogen occupies similar Bernal polyhedrons (tetrahedrons and octahedrons). Interstice diffusion factors in disordered material can be calculated as temperature and concentration function with hydrogen energies distribution and constant saddle point energy according to Kircheim formalism (Kircheim et.al, 1985).

$$D = D_0^1 \frac{\partial}{\partial C}\left\{(1-C)^2 \exp\left(\frac{\mu}{RT}\right)\right\}, \qquad D_0^1 = D_0^* \exp\left(\frac{E_0}{RT}\right) \tag{11}$$

Here D_0^* - pre-exponent factor, E_0- mean activation energy, equal to difference between mean Hydrogen energy, calculated, from energy distribution function and saddle point constant energy $E_0 - E_g$, (if energy distribution is Gaussian).

Hydrogen diffusion factors are calculated from equation (11) dependent on its concentration for amorphous $Pd_{83}Si_{17}$ alloy at T=298K temperature. It was obtained, that D_H increases depending on its concentration increase.

For example D_H value is $7.85 \cdot 10^{-6}$cm$^2 \cdot$s^{-1} at T=298K and C_H(H/Me)=10^{-3} for amorphous $Pd_{83}Si_{17}$ alloy.

Basing on D_H temperature dependence, diffusion activation energy value was estimated as E_0 = 18.9 kj/mol. It should be noted, that for crystal alloy activation energy is higher. It's equal to 26kj/mol independently on Hydrogen concentration.

According to Richards theory (Richards, 1983), there is Hydrogen probability to occupy low energy interstices, that are large faces polyhedrons.

Due to Hydrogen concentration increase, it occupies low energy interstices forcing H atoms to overcome higher energy potential barriers. Thus it neutralizes one of the factors, which decreases diffusion mobility.

On the other hand, Hydrogen atoms location in the higher energy interstices leads to activation energy decrease.

Described mechanism does not affect to diffusion, due to most part of Hydrogen atoms, absorbed by metal, have been found in low energy interstices (which are traps for H atoms). Sharp diffusion factor increase takes place only after traps saturation by Hydrogen.

6. Hydrogen diffusion in the amorphous Ni-Zr alloys

Computer calculation of the amorphous Ni-Zr and Ni-Zr-H alloys structure and properties are presented by fig. 10, 11 and table 2. The model system unlike (Pastukhov et.al, 2009, 2010) contained 640 (360)particles of nickel, 360 (640) particles of zirconium and 1(2) particles of hydrogen in the cubic cell. The movement equations integrating were carried out by time steps of $1.1 \cdot 10^{-15}$ s. General structure factors for $Ni_{64}Zr_{36}$ (alloy 1, curve 4) и $Ni_{36}Zr_{64}$ (alloy 2, curve 1), with Hydrogen and without it are presented on fig. 10. All curves have diffused interferential maxima proper to amorphous state, which indicates, that amorphous state is saved with Hydrogen absorption at low as well as at high hydrate-forming element and Hydrogen concentration in an alloy. Increasing the number of H - atoms in a MD model for 1- alloy initially results in structural factor peaks displacement to the low dispersion vectors (S) and in main peak height (h) increasing. Then the displacement vice versa results in the high S- and low h-values. It testifies to the quantity of H-atoms affects to amorphous alloys structure. All peaks of a(s) became more relief, oscillations extend to higher scattering vectors. The authors (Sadoc et.al, 1973, Maeda & Takeuchi 1979) proved, that icosahedrons type of atoms packing is dominating in amorphous metals structure, where high polyhedron concentration with coordination number 12 takes place. The main structural factor maximum height and form of the bifurcated second peak are determined by contacting polyhedrons quantity and their type of bond (Brine & Burton, 1979). The amorphous alloy short order therefore can be described with the help of a coordinating icosahedron cluster, which is the basic structural unit of $NiZr_2$ crystal.

Hydrogen in such a structure can be located in numerous tetra-cavities, formed by Ni and Zr atoms (Kircheim et.al, 1988). For 2 - alloy, that is close to $NiZr_2$ composition (curve 1), two first maxima location of a(s) curve corresponds to averaged location of the interference lines for crystal $NiZr_2$ compound. Hydrogen atom including in the MD-model (curve 2) leads to strong diffusion and height decreasing of relatively good resolved structure factor peaks due to Hydrogen penetration into numerous cavities of the amorphous structure. Hydrogen atoms probably form with Zr some kind of quasi crystal ZrH_2 lattice (Sudzuki et.al, 1987). This assumption reveals in a better resolution of short and long diffraction maxima (3, 6 curves) of structure factors for alloys with high contents of Zr and H atoms.

Partial $g_{ij}(r)$ radial distribution functions of model systems and short order parameters are presented in Fig. 11 and in the table 2. For all low and zero hydrogen alloys, the shortest inter-atomic distance of Ni-Ni pair remains constant (0.240nm), decreasing up to 0.230nm when H increases up to two atoms. Inter-atomic distances of N-Zr and Zr-Zr pairs considerably decrease with growth of Zr and H concentration. We note that rNi-Ni and rZr-Zr are close to Ni and Zr atoms diameters (0.244 nm and 0.324 nm) correspondently, and the distance between Ni-Zr atoms is somewhat less than the sum of the Ni and Zr atoms radii, that is confirmed by diffraction experiment results (Buffa et.al, 1992). This fact confirms bond formation between these elements due to hybridization of vacant 3d – electron band of Ni and 4d-band of Zr Hafiuer et.al, 1993). Calculated diffusion coefficients of hydrogen for amorphous Ni-Zr-H alloys are presented in the Table 2. The value of D_H varies from $2 \cdot 10^{-4}$ up to $1.2 \cdot 10^{-5} cm_2 \cdot s^{-1}$, in the same limits, as diffusion coefficients of H atoms in an icosahedron TiNiZr alloy (Morozov et.al, 2006). As it follows from the Table 2, D_H grows

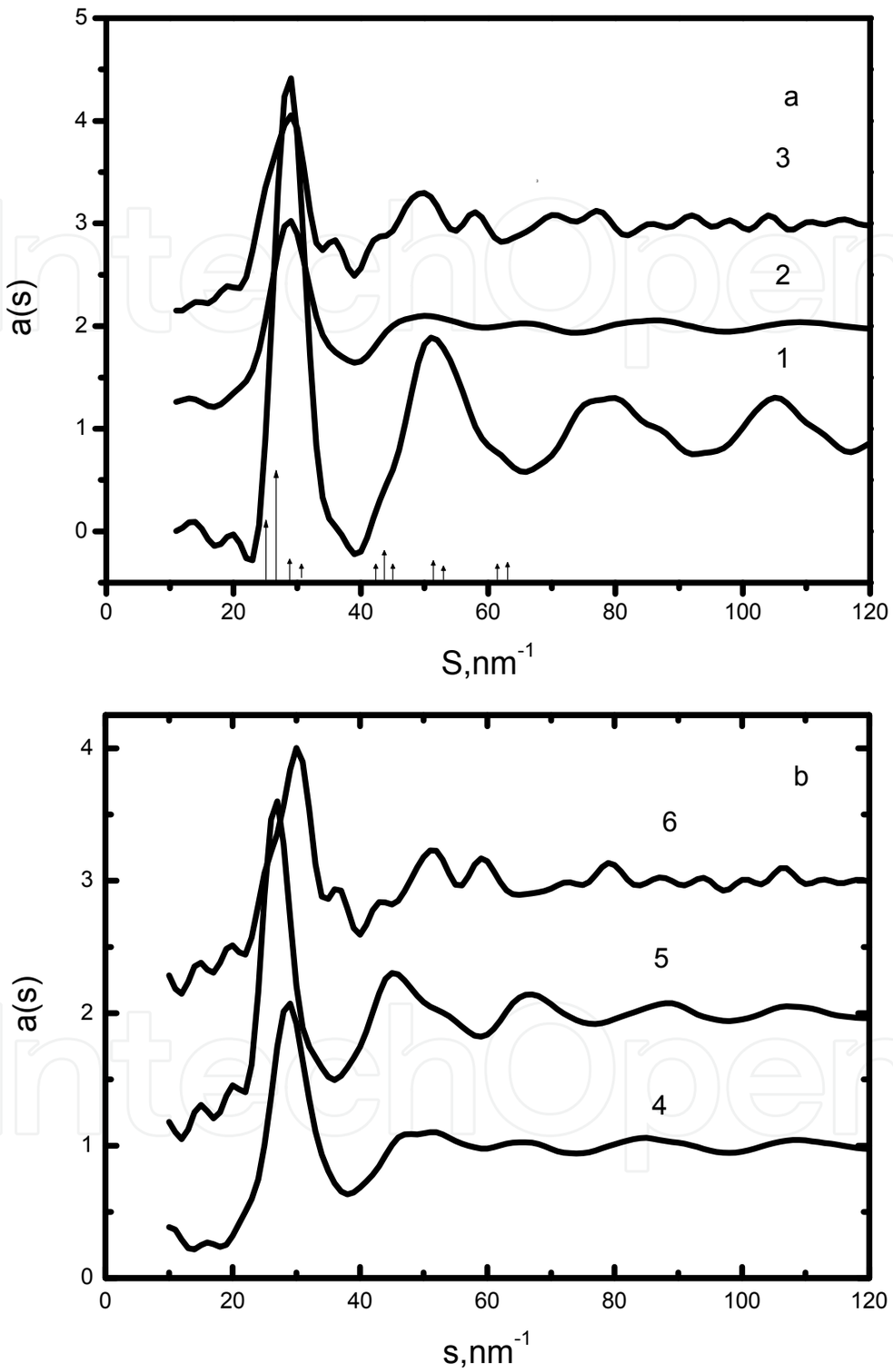

Fig. 10. Amorphous Ni-Zr alloys structure factors with hydrogen and without:
a) $Ni_{36}Zr_{64}$(1), $Ni_{36}Zr_{64}$+1H(2), $Ni_{36}Zr_{64}$+2H(3);
b)$Ni_{64}Zr_{36}$(4), $Ni_{64}Zr_{36}$+1H(5), $Ni_{64}Zr_{36}$+2H(6).

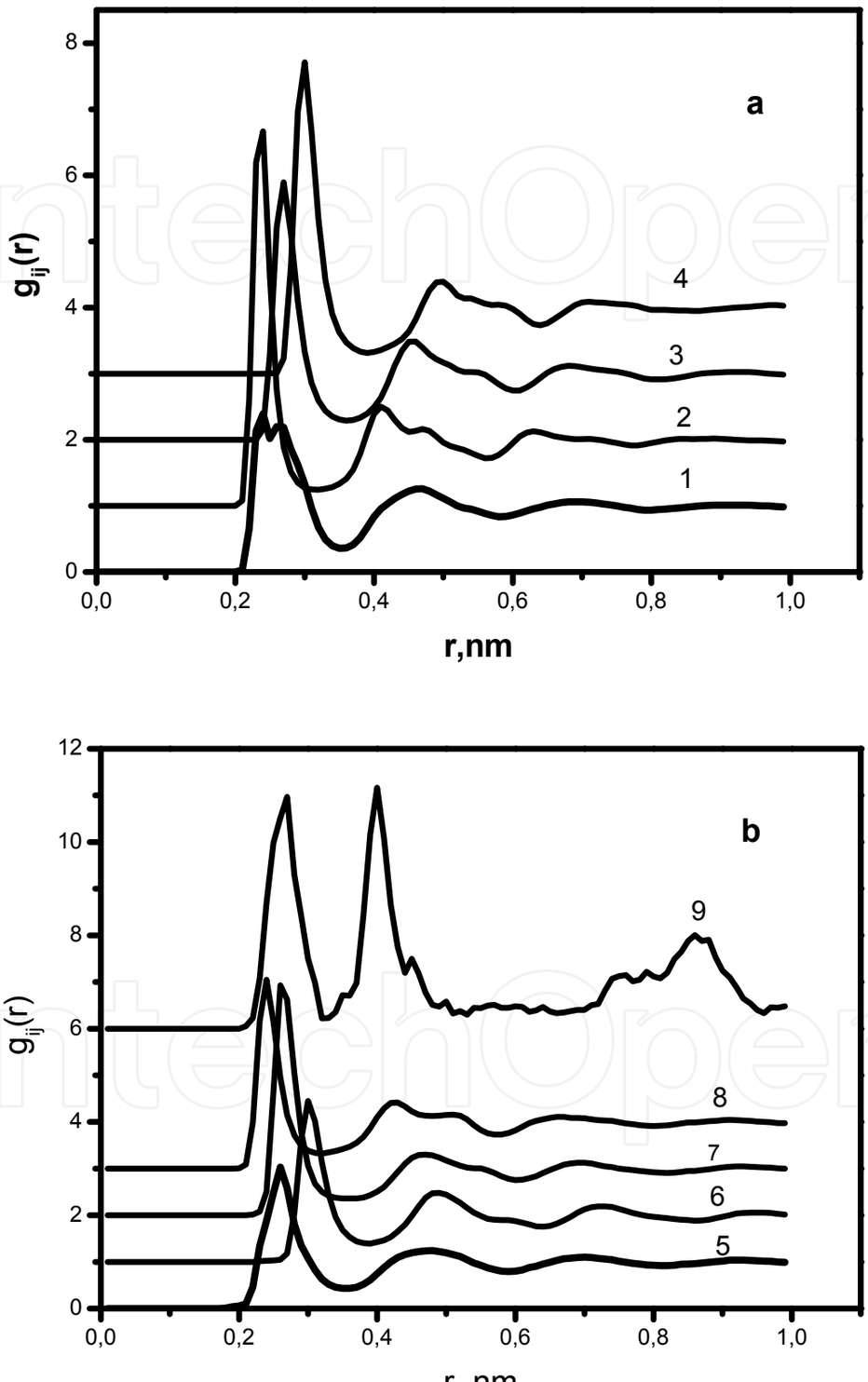

Fig. 11. Radial distribution functions g_{ij} (r) of $Ni_{64}Zr_{36}$ alloy: (a) - no hydrogen; (b) - one hydrogen atom. Partial g_{ij} (r): 1,5- general; 2,8 - Ni-Ni; 3,7 - Ni-Zr; 4,6 - Zr-Zr; 9 - H-H.

with increase of hydride forming element Zr concentration and H atoms in the MD-model. The activation energy of hydrogen diffusion for amorphous $Ni_{64}Zr_{36}$ alloy was estimated in the 298-768K temperature interval. A value of E=0.1eV was obtained. This result on H atoms diffusion may be explained by various energy position (Richards, 1983, Kircheim et.al, 1988) in the disordered materials. Deep potential wells acts like traps (octa-cavities) and are occupied by hydrogen initially. Then hydrogen occupies interstices with high energy values (tetra-cavities) and an abrupt increase of D_H is observed.

System	Partial RDF			D_H at 298K
	Ni-Ni	Ni-Zr	Zr-Zr	
	r, nm	r, nm	r, nm	cm^2s^{-1}
$Ni_{64}Zr_{36}$	0.238	0.270	0.301	
$Ni_{36}Zr_{64}$	0.240	0.261	0.290	
$Ni_{64}Zr_{36} < 1H_2 >$	0.240	0.266	0.310	$1.2 \cdot 10^{-5}$
$Ni_{64}Zr_{36} < 2H_2 >$	0.240	0.26	0.29	$1.7 \cdot 10^{-4}$
$Ni_{36}Zr_{64} <1H_2 >$	0.241	0.265	0.297	$8.9 \cdot 10^{-5}$
$Ni_{36}Zr_{64} < 2H_2 >$	0.230	0.250	0.280	$2.1 \cdot 10^{-4}$

Table 2. Short order parameters for amorphous alloy in the Ni-Zr and Ni-Zr-H systems.

7. Hydrogen and electric field effect to Iron impurities diffusion in the Zr-Fe melt

Iron and Zirconium diffusion factor dependence on electric field intensity and Hydrogen presence in the molten Zirconium had been analyzed in the terms of molecular dynamics (MD) method. Model system for research of Iron and Hydrogen ions behavior in the Zr-Fe-H melt at T=2273K temperature and electric field presence contained 516 Zirconium particles, 60 Iron particles and 1Hydrogen particle in cubic cell with a=2.44195 nm cube edge. Integration of the motion equation was carried out by $1.1 \cdot 10^{-15}$s time steps. Inter-particle potentials and its parameters had been taken from (Varaksin & Kozyaichev, 1991, Zhou et.al, 2001). Calculation results of impurities migration in the molten Zirconium are compared to experimental data (Lindt et.al, 1999, Ajaja et.al, 2002, Mimura et.al, 1995). Partial radial distribution functions $g_{ij}(r)$ for Zirconium-Iron melt are presented on fig. 12. Most probable inter-atomic distance in first coordination sphere is close to sum of atomic radii for Iron and Zirconium ($r_{Zr\text{-}Fe}$= 0.29nm, r_{Fe}= 0.130nm, r_{Zr}= 0.162nm).

This results comparison to computer simulation data for Ta-Fe melt (Pastukhov et.al, 2010, Vostrjakov et.al, 2010) reveals sufficiently close character of the radial distribution function for large dimension atoms, namely Ta-Ta (0.29 nm, r_{Ta} = 0.145nm) and Zr-Zr (0.324nm, r_{Zr}=0.162nm). Iron and Zirconium diffusion factors in the Zirconium melt in the presence, as well as absence of electric field and Hydrogen at 2273K had been calculated by means of MD method (fig. 13 and 14). Diffusion factor of Iron (D_{Fe}) in the Zirconium melts with Hydrogen linearly depends on electric field intensity (E) and Iron concentration (C_{Fe}). Hydrogen diffusion factor negligibly decreases from $2.16 \cdot 10^{-4}$ $cm^2 \cdot s^{-1}$ to $1.94 \cdot 10^{-4}$ $cm^2 \cdot s^{-1}$, if electric field intensity increases from 900 to 1020 v/m. Hydrogen inducing into system at $C_{Fe} \approx 0.1\%$ decreases D_{Fe} value from $7.86 \cdot 10^{-5}$ to $6.36 \cdot 10^{-5} cm^2 s^{-1}$, and electric field 1020 v/m intensity applying decreases D_{Fe} to $5.23 \cdot 10^{-5} cm^2 \cdot s^{-1}$ (fig.14).

Calculation results of D_{Fe} changing in dependence on E value had been compared to evaporation constant rate for the Fe-ions from Zr, calculated by equation (Pogrebnyak et.al, 1987, Vigov et.al, 1987)

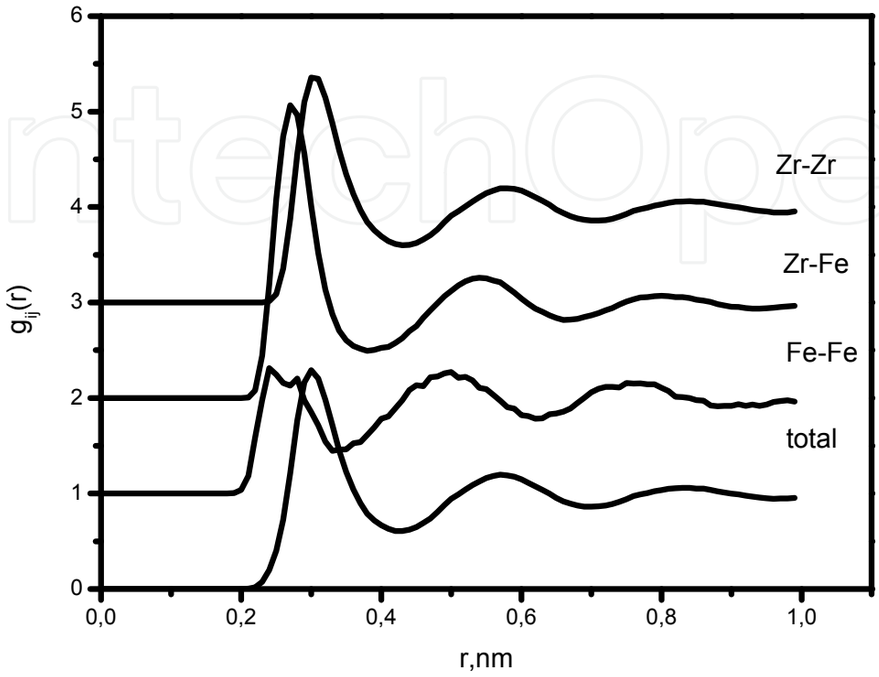

Fig. 12. Partial radial distribution functions $g_{ij}(r)$ for Zr-Fe melt at 2273K, calculated in terms of MD model.

$$k = \nu \cdot C_{Fe} \exp\left[-\frac{\lambda + I - W - (q^3 \cdot E)^{1/2}}{RT}\right], \tag{12}$$

where ν – ion vibration frequency (10^{13}·s^{-1}), C_{Fe} – impurity concentration, λ – Fe evaporation heat, I – first ionization potential (V/Å), E – electric field intensity, W – electron exit work, q – ion charge. Values of λ, I, W, R had taken in electron-volt, E – in volt per angstrom. Diffusion factor D directly depends on rate (*k*) and time (t) evaporation of main metal (Kuznetsov et.al, 1968). The log *k* and log D_{Fe} on E dependences (fig. 15) are relatively similar.

Thus assumption is possible, that limiting factor of Fe removal from the Zr melt is diffusion of Fe. The Hydrogen is considered as light intrusion impurity into metals with different cell type. Therefore Hydrogen diffusion is significant problem in researching of high temperature metals refining. Impurities have less action upon Incoherent diffusion. Therefore this kind of diffusion becomes dominating at high temperature (Maximov et.al, 1975).

We had compared Hydrogen diffusion factors in Ta at 3400K (Pastukhov et.al, 2010) and in Zr at 2273K (Ajaja et.al, 2002). This values are 1,7 10^{-5} and 5,01 10^{-4} cm^2·s^{-1} respectively. The authors (Maximov et.al, 1975) explain such difference due to Hydrogen diffusion activation energy (E_a) dependence on atomic metal mass, its Debye frequency, modulus of elasticity and volume change at Hydrogen addition.

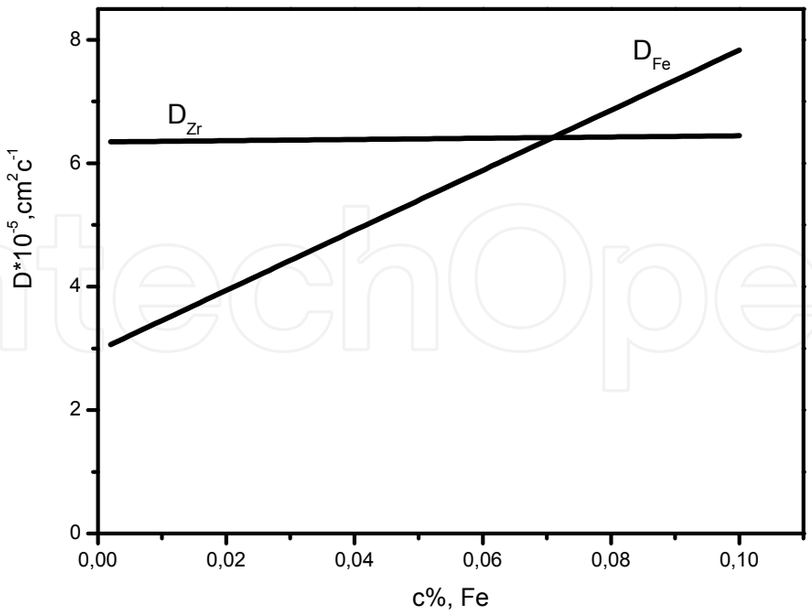

Fig. 13. Dependencies of D_{Fe} and D_{Zr} on Iron concentration at 2273K (MD - calculation).

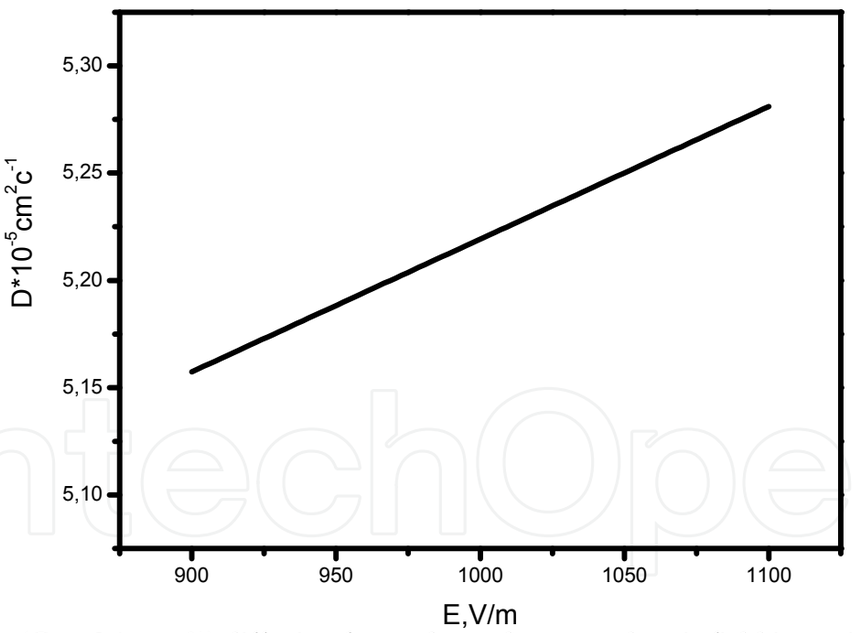

Fig. 14. Iron (C_{Fe} =0.1mas.%) diffusion factor dependence on electric field intensity at 1173K temperature (MD – calculation).

Calculated values of E_a for different metals (Flynn et.al, 1970) are in quantity agreement with experimental data. Temperature dependence D_H at high temperatures is described in the term of theory (Flynn et.al, 1970). Authors (Shmakov et.al, 1998) calculated D_H in Zirconium at 2273K without electric field influence as $3.862 \cdot 10^{-4} cm^2 \cdot s^{-1}$, which low differ from our calculated value $D_H = 5.01 \cdot 10^{-4} cm^2 \cdot s^{-1}$.

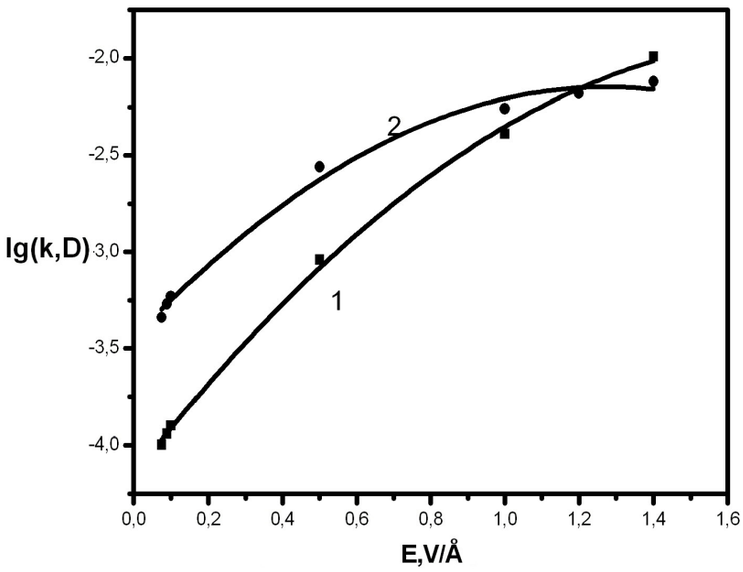

Fig. 15. Dependence of lgD_{Fe} (curve 1) and lgk (curve 2) on electric field intensity.

We have estimated diffusion layer thickness (x) by (13) equation (Flynn et.al, 1970). Calculation were carried out basing on C_{Fe} - experimental time – dependence (Mimura et.al, 1995). Value of D_{Fe} we calculated by MD – method.

$$C_{(x,t)} = C_0 erfc\left(\frac{x}{2\cdot\sqrt{D_{Fe}\cdot t}}\right), \tag{13}$$

In the equation C_0 and $C_{(x,t)}$ are impurity concentrations in initial and refined Zirconium (Flynn et.al, 1970) and t is time of refining. Calculated (*x)* value is equal $7\cdot10^{-2}$cm. By the order of value it's close to data on Silicon borating (Filipovski et.al, 1994), which is $1.6\text{-}1.8\cdot10^{-2}$cm. It should be noted, that zone thickness of Zirconium shell interaction with molten Uranium is $0.2\cdot10^{-2}$cm (Belash et.al, 2006).

We carried out calculation of Iron removal rate (G) from Zirconium by Iron concentration decrease during matched time intervals of plasma-arc-melting (PAM) with Hydrogen basing on the experimental data of (Mimura et.al, 1995) for 9.5 Pa and 50% of Hydrogen concentration in residual Argon. The data are shown in table 3. Mean residual Iron concentration at 15, 90 and 165 minutes of melting compiled 0.46, 0.01 and $2.2\cdot10^{-4}$ mas.% respectively. These calculations had been compared with Iron evaporation rate from Zirconium melt obtained from Langmuir equation:

$$L = 0.0583\gamma C_{Fe} cp\sqrt{\frac{M}{T}} \tag{14}$$

This equation parameters are following: Iron activity coefficient in Zirconium (γ) is equal to 0.052 from [43], (C_{Fe}) - concentration of Iron in Zr, (p) – Iron vapor pressure at 2273K, (M) – Iron atomic mass, (T) – Kelvin temperature. Temperature of melting [46] is indicated in the 2350 – 2450K limits. Calculation of L by these temperatures founds L < G in both cases. Ratio

G/L decreases at temperature increase. Obtained G/L ≈ 1.15 value at C_{Fe}= 0.46 and T = 2450K may indicate, that close to 15% of Iron is being removed due to electro-magnetic forces affect, rather than evaporation.

T,K	C_{Fe}, mas.%	logG	logL	G/L	Remark	Issue
2350	0.46	-4.572	-5.066	3.115	L<G	[4]
	0.01	-6.09	-6.728	4.348		
	$2.2\cdot10^{-4}$	-7.902	-8.386	3.047		
2450	0.46	-4.572	-4.755	1.153	L<G	[4]
	0.01	-6.09	-6.418	2.128		
	$2.2\cdot10^{-4}$	-7.902	-8.076	1.491		
2900	$7.82\cdot10^{-3}$	-6.967	-5.406	0.027	L>G	[2]
	$2.68\cdot10^{-3}$	-7.44	-5.871	0.027		
	$0.92\cdot10^{-3}$	-7.903	-6.335	0.028		
2450	$7.82\cdot10^{-3}$	-6.967	-6.525	0.361	L >G	[2]
	$2.68\cdot10^{-3}$	-7.44	-6.990	0.355		
	$0.92\cdot10^{-3}$	-7.903	-7.454	0.356		
2300	$7.82\cdot10^{-3}$	-6.967	-7.001	1.081	L < G	[2]
	$2.68\cdot10^{-3}$	-7.44	-7.466	1.062		
	$0.92\cdot10^{-3}$	-7.903	-7.930	1.065		

Table 3. Dependences of L and G on mean residual Iron content in Zirconium for PAM process. C_{Fe} – mean Iron concentration: initial (15min.), middle (90min.), and final (165min.) stage of melt.

8. Hydrogen and electric field effect to Iron impurities diffusion in Ta-Fe melt

Hydrogen and Iron atoms radial distribution functions and diffusion constants had been found by MD method in the Tantalum melt at 3400K in the presence and absence of outer electric field (fig. 16).

The model system was presented by 486 tantalum, 1 iron and 1hydrogen atoms in a cubic cell of 2.13572 nanometers cube edge length. Computer experiment data have found short order of Ta-Fe-H system at 3400K is close to Tantalum structure: first maximum at R_{Ta-Ta} ≈ 0.29 nm corresponds to Tantalum atom radius ≈ 0.292 nm. All RDF maxima diffusion is observed at electric field and Hydrogen in the Ta-Fe system. This fact may indicate liquid transition to more disordered structure.

Unusual kind of RDF curve for Ta-H atoms pairs obtained at electric field 1020v/m intensity (fig. 17): first maximum of the curve is bifurcated, besides first sub-peak at r_1 = 0.22nm corresponds to one of most probable distance Ta-H and second sub-peak at r_2 = 0.24nm corresponds to Ta-Fe without electric field.

Dynamics and local structure of the close to Hydrogen surrounding for the ternary interstitial alloy should depend on Hydrogen concentration, temperature and solvent structure short order. There is no conventional opinion about Hydrogen location in such systems. Since the Hydrogen atom radius is 0.032 nm, it can occupy octahedron (0.0606 nm), as well as tetrahedron (0.0328нм) (Geld et.al, 1985) location. System Ta – H particularity is

that starting from the concepts of geometry, distance between Tantalum atom and octahedron interstice centre in Tantalum cell more, than Ta (0.146nm) and H (0.032nm) radii sum. Distance Ta – H remains less than equilibrium distance, and Hydrogen not always occupies interstice centre.

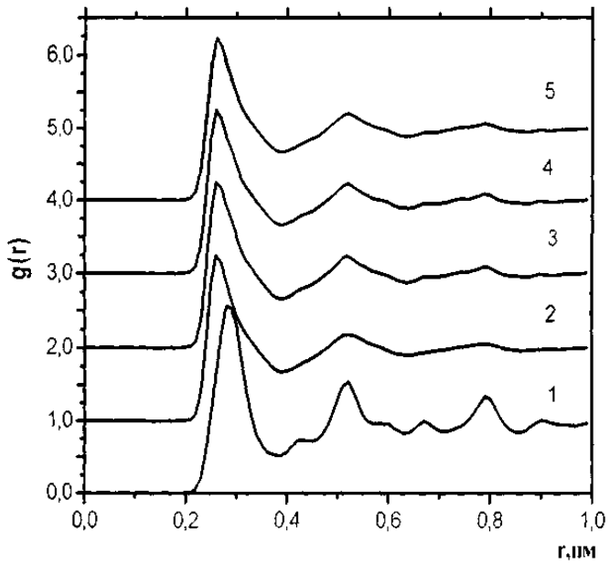

Fig. 16. Radial distribution function g (r) for Ta-Fe melt at 3400 K temperature, obtained in MD model at 15.4 g/sm^3 liquid Ta density. 1. No electric field, no hydrogen, 2. Electric field 85 [V/m], no hydrogen, 3. Hydrogen, no electric field, 4. Electric field 85 [V/m], Hydrogen, 5. Electric field 1020 [V/m], Hydrogen.

At the same time, distance from the octahedron interstice centre to the second neighbors, $R_2=a/\sqrt{2}=0.234$nm is more than Tantalum plus Hydrogen distance. That leads to Hydrogen atoms shift from octahedron centre to whatever neighbor of Tantalum atom.

Dynamics and local structure of the close to Hydrogen surrounding for the ternary interstitial alloy should depend on Hydrogen concentration, temperature and solvent structure short order. There is no conventional opinion about Hydrogen location in such systems. Since the Hydrogen atom radius is 0.032 nm, it can occupy octahedron (0.0606 nm), as well as tetrahedron (0.0328нм) (Geld et.al, 1985) location. System Ta – H particularity is that starting from the concepts of geometry, distance between Tantalum atom and octahedron interstice centre in Tantalum cell more, than Ta (0.146nm) and H (0.032nm) radii sum. Distance Ta – H remains less than equilibrium distance, and Hydrogen not always occupies interstice centre.

At the same time, distance from the octahedron interstice centre to the second neighbors, $R_2=a/\sqrt{2}=0.234$nm is more than Tantalum plus Hydrogen distance. That leads to Hydrogen atoms shift from octahedron centre to whatever neighbor of Tantalum atom.

Hydrogen shift from geometric centre of octahedron position during heating of researched system is possible. According to computer experiment data, distance between nearest Tantalum and Hydrogen atoms changes at electric field and Hydrogen presence, but Ta-Fe remains constant (table 4).

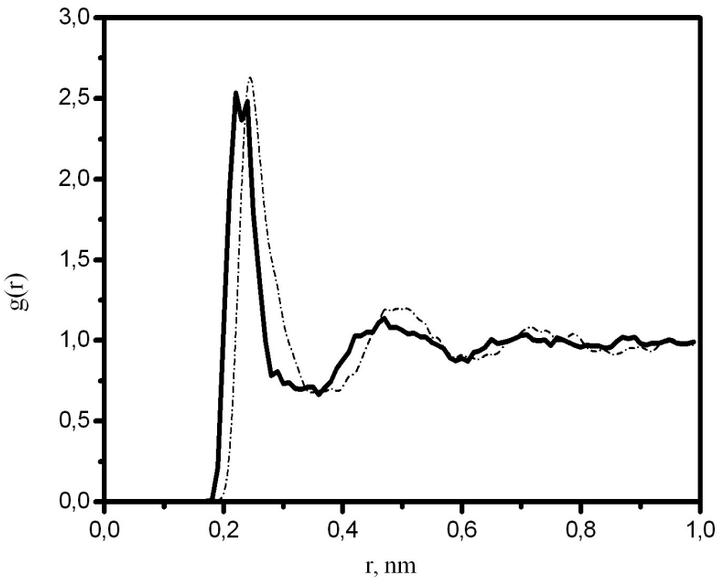

Fig. 17. Partial distribution function of the atomic Ta-H pair in electric field 1020 v/m (dashed curve) and Ta-Fe without electric field (solid curve), obtained by MD model.

After Hydrogen induction into MD cell, Tantalum diffusion constant increases from $1.7 \cdot 10^{-4}$ до $7. \cdot 10^{-4}$ cm^2 s^{-1}, which some less, than Iron diffusion constant increase: from $1.3 \cdot 10^{-5}$ to $1.5 \cdot 10^{-4} cm^2$ s^{-1}.

Thus, Hydrogen increases Iron atoms mobility more than electric field. This fact is in god agreement with Ta-H and Ta-Fe bonds strength.

System	T, K	E,V/m	PRDF (nm)		
			rTa-Ta	rFe-Fe	rTa-H
Ta-Fe	3400		0.29		
Ta-Fe-H	3400	85	0.26	0.25	
Ta-Fe-H	3400		0.26	0.24	0.22
Ta-Fe-H	3400	85	0.26	0.24	0.235
Ta-Fe-H	3400	1020	0.26	0.24	0.22/0.24

Table 4. Partial inter-atomic distances in the Ta-Fe by MD calculation.

9. Conclusion

Amorphous and liquid systems structure for Fe, Pd, Zr, Ta, Si with presence and absence of Hydrogen atoms had been researched by means of x-rays diffraction and molecular dynamic methods. Strong affect of H atoms to amorphous matrixes Fe-Ni-Si-b-C-P, Pd-Si and Ni-Zr structure had been obtained.

Observed RDF changing at Hydrogen presence had been revealed in better resolution of the close and distant maxima could indicate to stable hydride bonds like Pd-H, Si-H, Zr-H formation.

Calculated by MD model Hydrogen diffusion constants increase on H concentration and hydride forming element presence in alloy (system Ni-Zr-H). Not only amorphous alloy

component (Pd-Si-H) affects to H atoms mobility, but Hydrogen atoms can considerably change other components (Si) diffusion. Refining processes of the liquid high-melting metals, like Zr, Ta, containing Fe impurities can be analyzed by MD method for PAM and EBM melting technologies. The method gives opportunity to estimate limiting stage of process, electric field affect and Hydrogen presence in system to Fe diffusion constant in the melts.

The researches had been carried out with financial support of Minobrnayka. Federal contract 16.552.11.7017, science equipment of CKP "Ural-M" had been used.

10. References

Ajaja, V.; Vugov, P. & Lavrinenko, S. et. al. (2002). Electron-beam melting of Titanium, Zirconium and Hafnium. *Voprosi atomnoi nauki I tehniki*. (2002). No. 6. pp. 95-99

Alder, B. & Wainwright, T. (1959). Studies in Molecular Dynamics. I. General Method - *J. Chem. Phys.* Vol.31, No.2, pp. 459-469.

Avduhin, V.; Katsnelson, A. & Revkevich, G. (1999). Oscillatory phase transformations in the initial relaxation stage of Pd-Er-H alloy *Crystallography* (1999), Vol.44. No.1.p.49; (1999). Non equilibrium phase transformations of oscillatory type in Pd-Er alloy, relaxing after Hydrogen saturation. *Vectnik Moscow Univercity* Ser.3 (1999). Vol.40. No.5. p.44.

Belash, N.; Tatarinov, V. & Semenov, N. (2006). Complex alloying of Uranium in centrifugal casting in Zirconium form. *Voprosi atomnoy nauki i tehniki. Seriya «Fizika radiatsionnih povrejdeni I radiatsionnoe materialovedenie».* (2006). No. 4. pp. 123-127

Brine, C. & Burton, Y. (1978). Icosahedral Microclusters. A Possible Structural Unit in Amorphous Metals. *Phys.Stat. Sol.(b).* (1978). Vol. 85. No.1. pp.393-402

Buffa, F.; Corrias, A.: Licheri, G.; Navarra, G. & Raoux, D. (1992). Short range structure of mechanically alloyed amorphous Ni_2Zr investigated anomalous X-ray scattering. *J. Non-Cryst. Solids*, Vol.150. Issues 1-3, 2 November (1992). pp. 386-390

Filipovski, F. & Nasarenko, I. (1994). Method for removing suicide coatings in a medium of low-melting Metals. *Materials Science.* (1994).Vol.30. No.3. pp.368-370

Flynn, C. & Stoneham, A. (1970). Quantum Theory of Diffusion with Application to Light Interstitials Metals. *Phys Rev* (1970). B1. pp. 3966-3978.

Gordeev, V.; Popov, A. & Filikov, V.(1980). Structure of amorphous Silicon, obtained by high frequency ion-plasma spraying. *Izv. AN.USSR. Neorgan. materiali.* 1980. Vol.16. No.10, pp. 1733-1736.

Gabis, I. (1997). Transfer of Hydrogen in the graphite films, amorphous Silicon and Nickel oxide. *Phizika* i tehnika *Poluprovodnikov*. 1997. Vol.31. No. 2, pp. 145-151.

Geld, P.; Ryabov, R. & Mokhracheva. (1985). Vodorod I fizicheskie svoystva metallov I splavov. Nauka. (1985), Moscow. Russia.

Grashin, S.; Sokolov, U. & Gorodetsky, A. et. al. (1982). Hydrogen interaction with material of discharge tokamak chamber. *Preprint IAE (rus.)* No.3622/7. Moscow. 1982.

Hafiuer, J.; Krajci, M. & Hausleitner, C. (1993). Methods in the determination of partial structure factors. *Scientific Publishing.* (1993). Singapore

Herst, D. (1962) Diffusion of fusion gas. Calculated diffusion from sphere taking into account trapping and return from the traps. *In CRRP -1124. Atomic Energy of Canada Inst. Conf*. Oct.-Nov., 1962, Balk River. pp. 129- 135

Ivanova, V.; Balankin, A.; Bunin, I. & Oksogoev, A. (1994). *Sinergetica i fractali v materialovedenii*. Nauka. (1994).Moscow, Russia

Kirchheim, R.; Sommer, F. & Schluckebier, G. (1982). Hydrogen in amorphous metals. *J. Acta Metall.* (1982) Vol.30. No.6. pp. 1059-1068

Kichheim, R.; Szokefalvi-Nagy.; Stolz, A. & Spelling, A. (1985). Hydrogen in deformed and amorphous palladium – silicon ($Pd_{80}Si_{20}$) compared to hydrogen in deformed and crystalline palladium. *J. Non-Cryst. Solids*. (1985). Vol. 70. No.2. pp. 323-329

Kircheim, R. et al. (1988). Hydrogen in amorphous and nanocrystalline metals. *Mat. Sci. Eng*. (1988). Vol.99. No.2, pp. 457-462

Kuznetsov, V.; Loginova, R.; Ovsyanikov, M. & Postnikov, V. (1968). *Growth and structure processes of mono-crystal Semiconductors.* Part I. Nauka. (1968). Novosibirsk. Russia.

Lifshits, A. (1976). Interaction of the membranes with nonequilibrium gases in the case of adsorption with dissociation. *JTF (Jurnal Teoreticheskoy Fiziki (rus.)).* Vol.46, No.2, pp. 328 – 338.

Lindt, K.; Muhachev, A.; Shatalov, V. & Kotsar, M. (1999). Perfection of process of calcium-thermal reduction of Zirconium tetra-fluoride. *Voprosi atomnoy nauki i tehmiki. Seriya «Fizika radiatsionnih povrejdeni I radiatsionnoe materialovedenie».* (1999). No. 2. pp. 3-8

Maeda, K. & Takeuchi, S. (1979). Geometrical characterization of Computer Constructed Metallic Amorphous Structure *Techn.,Rep. ISSP(a)*. (1979). No.54. pp.1-17

Maksimov, E. & Pankratov, O. (1975). Hydrogen in metals. *Uspehi fizicheskih nauk. (UFN).* (1975). Vol. 116. Issue 3. pp. 385-412.

Mimura, K.; Lee S. & Isshiki M. (1995). Removal of alloyng elements from zirconium alloys by hydrogen plasma-arc Melting. *Journal of Aloys and Compounds.* (1995). Vol. 221. pp. 267-273

Morozov, A.; Isaev, E. & Vekilov, U. (2006). *Fizika tverdogo tela (rus.).* (2006). Vol. 48. Issue 9. pp. 1537-1540

Pastukhov, E.; Sidorov, N.; Belyakova, R. & Polukhin, V. (1988). Hydrogen affect to electric resistance of amorphous films Pd-Si and Fe-B in crystallization temperature interval. *Abstracts of III Vsesouznoy conference "Problems of amorphous metallic alloys researches"(rus.)*. Moscow, pp. 27-28.

Pastukhov, E.; Vatolin, N. & Lisin, V. et. al. (2003). *Diffractsionnie issledovaniya stroeniya visokotemperaturnix Rasplavov*. UrO RAN. Ekaterinburg. Russia.

Pastuchov, E.; Sidorov, N. & Chentsov, V. (2007). Diffusion permeability of hydrogen in amorphous Fe-Ni-Si-B-C-P alloy The optimization of the composition, structure and properties of metals, oxides, composites, nano-and amorphous materials. *Proceeding of the VII International Russia-Israeli Conference*, June 24-28, Jerusalem 2007, pp. 85-94.

Pastukhov, E.; Sidorov N. & Chentsov, V. (2008). Hydrogen affect to short order structure of liquid amorphous and crystal Silicon. *Proceedings of IX Russian seminar "Computer simulation of glasses and melts physical-chemical properties."* Kurgan. Russia. (2008). pp.25-26.

Pastukhov, E.; Sidorov,V.; Polukhin, V. & Chentsov, V. (2009). Short Order and Hydrogen Transport in Amorphous Palladium Materials. *Defect and Diffusion Forum.* Vols.283-286 (2009) pp.149-154

Pastukhov, E.; Vostrjakov, A.; Sidorov,V.; & Chentsov, V. (2010). Molecular Dynamic Calculation of Hydrogen and Iron Diffusion in molten Tantalum under Electric Field. *Defect and Diffusion Forum*. Vols.297-301 (2010) pp.193-196

Pogrebnyak, A.; Kulmentyeva, O. & Kshnyakin, V. et. al. (2002). Strengthening and mass transport in impulse-plasma-detonation of steel treatment. *Fizika i himiya obrabotki materialov*. (2002). No. 2. pp. 40-48

Polukhin, V.; Pastukhov, E. & Sidorov, N. (1984). Structure of $Pd_{1-x}Si_x$ and $Fe_{1-x}P_x$ alloys in liquid and amorphous states. *Phizika metallov i metallovedenie (rus.),* Vol.57, No.3, pp. 621-624.

Polukhin, V. & Vatolin, N. (1985). *Modelirovanie Amorfnih Metallov (rus.),* Nauka, Moskow, USSR

Polukhin, V.; Vatolin, N.; Belyakova, R. & Pastukhov, E. (1985). Hydrogen affect to amorphous Iron distribution function from molecular dynamic simulation. *Dokladi AN SSSR (rus.)*. Vol.287, No.6, pp. 1391-1394.

Polukhin, V.; Sidorov, N. & Vatolin, N. (1997). Statistic models of diffusion and permeability of Hydrogen in the membrane amorphous alloys. *Melts (Rasplavi (rus.))* No.3, pp. 3-27

Panzarini, G. & Colombo, L. (1994). Hydrogen Diffusion in Silicon from Tight-Binding Molecular Dynamics. *Phys. Rev. Lett.* (1994), No.73, p. 1636

Rappe, A.; Cascwit, C. & Cowell, K. (1992). UFF, a full periodic Table force field for molecular mechanics and molecular dynamics simulations. *J. Am. Chem. Soc*, Vol.114, No.25, pp. 10024-10035.

Richards, P.; (1983). Distribution of activation energies for impurity hopping in amorphous metals. *Phys.Rev.* (1983). Vol.27. No. 4. pp. 2059-2072

Sadoc, J.; Dixmier, J. & Guiniter, A. (1973). Theoretical Calculation of Dense Random Packing of Equal and Non-equal Size Hard Spheres. Application to Amorphous Metallic Alloys. *J.Non-Cryst.Solids*. Vol.12. No.1.(1973). pp.46-60

Shmakov, A. & Singh, R. (1998). Some peculiarities of Hydrogen behavior and related hydride cracking in zirconium based reactor alloys. *Atomic Energy*.(1998). Vol.85. No.3. pp.675-678

Sidorov, N. & Pastukhov, E. (2006). Hydrogen diffusion in an amorphous Palladium: molecular-dynamic model. *Proceedings of the Third Russian conference "Physical problems of Hydrogen energetics"*. Sanct-Peterburg. Russia. 20-22 November. (2006). pp. 39-41.

Sokolov, U.; Gorodetsky, A.& Grashin, S. et. al. (1984). Interaction of hydrogen with the material of discharge chamber of tokamak TM-4

Stillimger, F. & Weber, T. (1985). Computer simulation of local order in condensed phases of silicon. *Phys.Rev.* B31, (1985). pp. 5262-5271.

Sudzuki, K.; Fudzinori, H. & Hasimoto, K. (1987).*Amorfnie metalli.* (1987). Metallurgiya. Moskow. Russia

Tersoff, J. (1986). New empirical model for the structural properties of silicon. *Phys. Rev., Lett.* No.56. (1986) .pp. 632-638

Varaksin, A.; Varaksin, A. & Kozyaichev, V. (1991). Diffusion of Hydrogen in Palladium: Molecular dynamics Simulation. *Phizika metallov i metallovedenie (rus.),* Vol.57, No.2, pp. 45-51.

Vatolin, N.; Poluhkin, V.; Belyakova, R. & Pastukhov, E. (1988). Simulation of the Influence of Hydrogen on the Structural Properties of Amorphous Iron. *Mater. Science and Eng*. (1988). No.99. pp. 551-554.

Vatolin, N.; Polukhin, V.; Belyakova, R.; Pastukhov, E. & Sidorov, N. (1989).The properties and thermostability of the hydrated glasses based on Iron and Palladium. *Abstracts of international congress on glass.* Leningrad. Nauka. pp. 378-381.

Verlet, L. (1976). Computer experiments in classical fluids. – *Phys. Rev*. Vol.159, No.1, pp.98-103.

Vigov, P.; Goncharov, K. & Kuzmenko, V. et.al. (1987). *Poly-elements activation analysis by means of (p,n)-reactions*. HFTI. (1987).Kharkov. AN Ukr.SSR.

Vostriakov, A.; Sidorov, N.; Pastukhov, E. & Lisin, V. (2010). Influence of the Electric Field Strength and Hydrogen on the Rate of Removal of Iron Atom Impurites in Refinig Remelting of Tantalum. *Russian Metallurgy (Metalli).* Vol. 2010, pp.124-127

Zhou, X.; Wadly, H.; & Johnson, R. (2001). Atomic scale structure of sputtered metal multilayers. *Acta mater*. No.49, pp. 4005-1015.

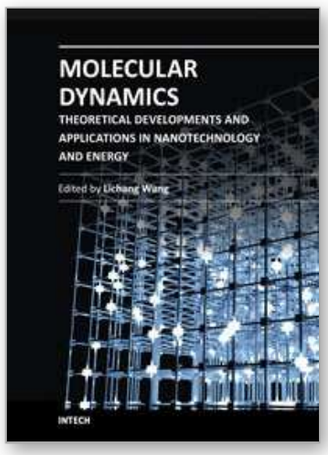

Molecular Dynamics - Theoretical Developments and Applications in Nanotechnology and Energy

Edited by Prof. Lichang Wang

ISBN 978-953-51-0443-8
Hard cover, 424 pages
Publisher InTech
Published online 05, April, 2012
Published in print edition April, 2012

Molecular Dynamics is a two-volume compendium of the ever-growing applications of molecular dynamics simulations to solve a wider range of scientific and engineering challenges. The contents illustrate the rapid progress on molecular dynamics simulations in many fields of science and technology, such as nanotechnology, energy research, and biology, due to the advances of new dynamics theories and the extraordinary power of today's computers. This first book begins with a general description of underlying theories of molecular dynamics simulations and provides extensive coverage of molecular dynamics simulations in nanotechnology and energy. Coverage of this book includes: Recent advances of molecular dynamics theory Formation and evolution of nanoparticles of up to 106 atoms Diffusion and dissociation of gas and liquid molecules on silicon, metal, or metal organic frameworks Conductivity of ionic species in solid oxides Ion solvation in liquid mixtures Nuclear structures

INTECH
open science | open minds

InTech Europe
University Campus STeP Ri
Slavka Krautzeka 83/A
51000 Rijeka, Croatia
Phone: +385 (51) 770 447
Fax: +385 (51) 686 166
www.intechopen.com

InTech China
Unit 405, Office Block, Hotel Equatorial Shanghai
No.65, Yan An Road (West), Shanghai, 200040, China
中国上海市延安西路65号上海国际贵都大饭店办公楼405单元
Phone: +86-21-62489820
Fax: +86-21-62489821

IntechOpen